RSC Advances

PAPER

View Article Online
View Journal | View Issue

Cite this: *RSC Adv.*, 2015, **5**, 15695

Flexible organic field-effect transistors with high-reliability gate insulators prepared by a room-temperature, electrochemical-oxidation process

Sheng Sun, Linfeng Lan,* Peng Xiao, Zhenguo Lin, Hua Xu, Miao Xu and Junbiao Peng*

Received 15th December 2014
Accepted 28th January 2015

DOI: 10.1039/c4ra16409a

www.rsc.org/advances

Flexible organic field-effect transistors (OFETs) with electrochemically oxidized gate insulators (AlO_x:Nd) covered by a thin layer of hydroxyl-free poly(perfluorobutenylvinylether) known as Cytop were fabricated on a polyethylene naphthalate (PEN) substrate. The AlO_x:Nd/Cytop bilayer insulator exhibited excellent insulating properties with low leakage current, high dielectric constant, high breakdown field, and low surface roughness. The pentacene film on AlO_x:Nd without Cytop consisted of small grains, while the one on AlO_x:Nd with Cytop exhibited a dendritic structure with a larger average grain size of ~350 nm. The pentacene OFET with Cytop exhibited higher mobility (0.75 $cm^2\ V^{-1}\ s^{-1}$) and better electrical stability under gate-bias-stress (in air condition) compared to that without Cytop. In addition, the flexible OFET was able to maintain a relatively stable performance under a certain degree of bending.

Introduction

Recently, organic field-effect transistors (OFETs) have attracted great attention due to their advantages of low cost, large area, and flexibility.[1–4] OFETs are considered as promising candidates for the back plane of flexible displays, and the application area is being enlarged to various sensing devices for temperature, liquid, gas, pressure, light, and biochemical materials.[5–9] To take advantage of their flexible nature and low-cost roll-to-roll technology, OFETs should be fabricated on flexible substrates. However, the handling and processing of flexible, plastic substrates will encounter a number of manufacturing challenges. For instance, the gate insulators compatible with the flexible substrates are much more limited than those compatible with the rigid substrates. Traditional inorganic insulators, such as SiO_2, require high temperatures. Insulating polymers are commonly used as the gate insulator of flexible OFETs for their good mechanical flexibility and solution-processibility, but most of them have relatively low dielectric constants, leading to a high operation voltage (≥50 V). Moreover, most of the insulating polymers have high leakage current as well as problems in long-term reliability and stability.

Al_2O_3 prepared by electrochemical oxidation (anodization) has attracted attention for its high dielectric constant (8–12), low leakage current, room-temperature and environmental friendly process, and low cost.[10–12] It seems that anodization is an ideal method for preparing gate insulators on flexible substrates, because of its room-temperature process. However, it is difficult to prepare anodic Al_2O_3 thicker than 10 nm directly on flexible substrates, because the Al film is easy to lose its covering in the form of flakes, peelings, or bubbles during anodization.[13] This phenomenon may arise from the poor contact between the Al film and the flexible substrate, or relatively high the water permeability of the flexible substrate. Meanwhile, the hillock formation characteristic of the Al film makes the devices unreliable. Employing Al foils on the flexible substrates can avoid these problems,[14,15] but they are very thick and can hardly be patterned by photolithography. Therefore, anodic Al_2O_3 on Al foils is difficult to apply to the back plane of the flexible displays.

In this paper, we managed to fabricate pentacene OFETs gated by anodized Al alloy (Al–Nd) at room temperature on flexible polyethylene naphthalate (PEN) substrate. Pentacene was selected as the semiconductor layer because it is one of the most widely studied organic semiconductors and therefore serves as a good point of ref. 16. To attain high mobility and good bias stability, a thin hydroxyl-free poly(perfluorobutenylvinylether) commercially known as Cytop layer was inserted between the active layer and the anodized gate insulator. The engineering of the organic/insulator interface was studied in detail.

Experimental section

The schematic diagram of the flexible pentacene OFET on the PEN substrate is shown in Fig. 1(a). The PEN substrate was attached to the same size glass carrier (conventional alkali-free glass).[17] A 300 nm thick Al–Nd (3 wt%) alloy gate electrode was

State Key Laboratory of Luminescent Materials and Devices, South China University of Technology, Wushan Road 381#, Tianhe District, Guangzhou, China. E-mail: lanlinfeng@scut.edu.cn; psjbpeng@scut.edu.cn

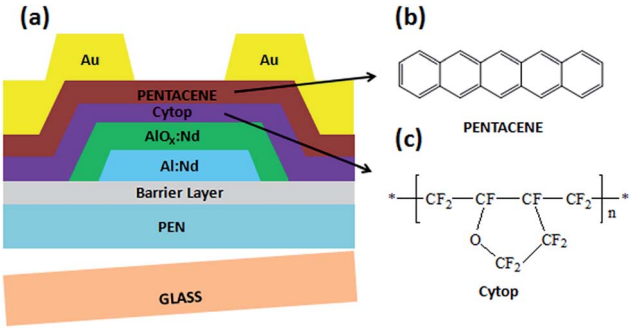

Fig. 1 Schematic diagram of the flexible OFETs (a), chemical structures of pentacene (b) and Cytop (c).

prepared by sputtering on the barrier layer and the gate metal array was patterned using conventional photolithography. Then, Al–Nd film was anodized to produce a layer of 200 nm-thick AlO_x:Nd on the surface of the Al–Nd film as the gate insulator.[18–20] Then, a 40 nm thick Cytop layer (CTL-809M from Asahi Glass, Fig. 1(c), dissolved in CT-Solv.180 in the ratio ~1 : 5) was spin-coated on the AlO_x:Nd layer. The capacitivity (C_i, use to extract the carrier mobility) of AlO_x:Nd and AlO_x:Nd/Cytop was 42 nF cm^{-2} and 22 nF cm^{-2}, respectively. After that, a layer of 80 nm-thick pentacene (99.995% purity Aldrich, Fig. 1(b)) film was thermally evaporated onto the insulator at room temperature under a vacuum pressure of ~3 × 10^{-4} Pa with a deposition rate of 0.1 Å s^{-1}. For the source/drain electrodes, a 50 nm-layer of Au was thermally evaporated through a shadow mask, defining a channel width/length (W/L) of 500/70 μm. All the electrical property of the OFETs was measured by using a semiconductor parameter analyzer (Agilent 4155C) and a probe station at room temperature in air atmosphere.

Results and discussion

To suppress hillock formation and reduce the surface roughness, Al–Nd was used as the gate instead of pure Al. There were not any flakes, peelings, or bubbles during anodization even at a thickness of as high as 200 nm. This is very important for the reliability of the insulator. The leakage current density was only ~10^{-7} A cm^{-2} at a field of as high as 3.0 MV cm^{-1}, which was lower than those of many other high-κ dielectrics.[21] Moreover, the breakdown field of these films was as high as ~6 MV cm^{-1}.

Although the anodic AlO_x:Nd has good insulating properties, the hydroxyl groups on the surface and the relatively high surface roughness are the two main drawbacks for OFET applications. To solve these problems, a thin Cytop layer was inserted between AlO_x:Nd and pentacene. Cytop is a type of hydroxyl-free, highly-hydrophobic insulating material. This fluoropolymer can easily form uniform thin-films from solution by spin-coating.[22,23]

The roughness of gate insulator is believed to reduce mobility in organic semiconductors due to the disorder induced in the accumulation order. The surface roughness of the insulator has important effect on the pentacene grain size, and can disturb π–π stacking, which is critical to efficient charge transport.[24] The root mean square (RMS) roughnesses of AlO_x:Nd without and with Cytop were evaluated by atomic force microscope (AFM) to be 4.1 and 1.4 nm respectively. The surface roughness of insulator reduced after Cytop covering, as expected.

Fig. 2 shows the output and transfer characteristics for OFETs with and without Cytop. OFETs without Cytop exhibited a field-effect mobility (μ) of 0.11 cm^2 V^{-1} s^{-1}, a turn-on voltage (V_{on}) of −4 V, and an on/off current ratio (I_{on}/I_{off}) of ~2.8 × 10^5; while the one with Cytop exhibited a higher μ of 0.75 cm^2 V^{-1} s^{-1}, a lower V_{on} of 0 V, and a higher I_{on}/I_{off} of ~2.0 × 10^6. Higher I_{on}/I_{off} for OFET with Cytop was ascribed to the higher mobility (resulting in higher I_{on}) and lower gate leakage current (resulting lower I_{off}). The properties of the pentacene OFET with and without Cytop layer were summarized in Table 1.

The performance enhancement by Cytop modification was ascribed to the changes of surface roughness, surface energy, and pentacene film geometry. To evaluate the surface energy of AlO_x:Nd with and without Cytop, water contact measurement was performed. Fig. 3(a) and (b) show the water contact angle measurement images of AlO_x:Nd and AlO_x:Nd/Cytop, respectively. The water contact angle for AlO_x:Nd was 66°, showing hydrophilic characteristic which was originated from the hydroxyl groups on the surface. After coated with Cytop, the water contact angle increased to 106°. According to the Young's equation,[25] the surface energy was greatly reduced by Cytop modification. In general, low surface energy is in favour of the enhancement of carrier mobility in pentacene OFET.[26]

Fig. 4(a) and (b) show the AFM images of pentacene films on AlO_x:Nd and AlO_x:Nd/Cytop, respectively. The grain size on

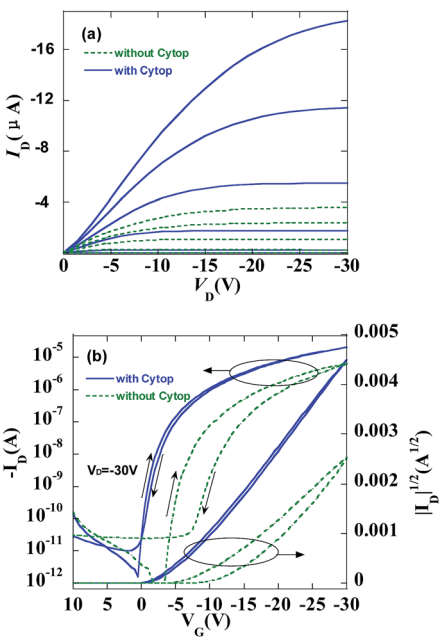

Fig. 2 Output (a) and transfer (b) characteristics of pentacene OFET with and without Cytop. The output curves were recorded at V_G = −30, −24, −18, −12, −6 and 0 V from top to bottom for either device, and the curves at lower V_G were overlapped from each other.

Table 1 Summary of properties of the pentacene OFET without and with Cytop layer

	μ ($cm^2\ V^{-1}\ s^{-1}$)	V_{on} (V)	I_{on}/I_{off}	Hysteresis (V)
Without Cytop	0.11	−4	2.8×10^5	3.9
With Cytop	0.75	0	2.0×10^6	0.6

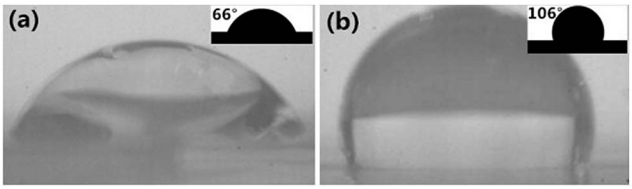

Fig. 3 Water contact angle measurement images of (a) AlO_x:Nd, (b) AlO_x:Nd/Cytop.

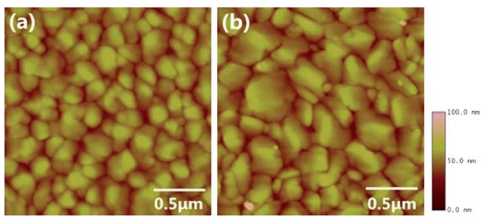

Fig. 4 AFM images of 80 nm thick pentacene films on (a) AlO_x:Nd, and (b) AlO_x:Nd/Cytop.

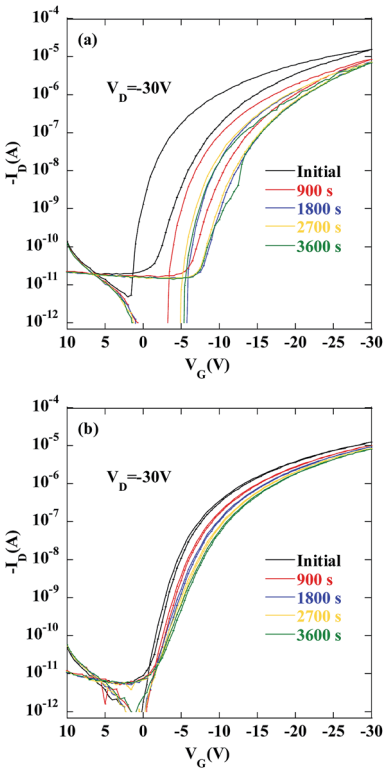

Fig. 5 The time-dependent transfer property under negative gate bias stress for pentacene OFET without (a) and with (b) Cytop. Stress condition: $V_G = -30$ V, $V_D = -30$ V. Every curve includes forward (left) and reverse (right) sweeps.

AlO_x:Nd with Cytop was much larger than that on AlO_x:Nd without Cytop. The pentacene on AlO_x:Nd without Cytop consisted of large numbers of small grains with an average grain size of ~200 nm, while the pentacene on AlO_x:Nd modified with Cytop exhibited a dendritic structure with an average grain size of ~350 nm. The changes in pentacene film morphologies were attributed to the changes of the surface roughness after Cytop modification, which was consistent with the results reported elsewhere.[27] Another reason for the performance improvement after Cytop insertion is the low dielectric constant of Cytop. It is known that if the insulator/semiconductor interface is more polar, the density of states (DOS) broadening becomes more severe, leading to more tail states, and carriers face a high potential barrier for upward hops into denser sites that lie closer.[22] Therefore, the OFET with Cytop can get better performance due to the reduction of the energetic disorder at the insulator/semiconductor interface and the facilitation of the carrier transport.

It is worth noting that the Cytop-modified OFET exhibited much smaller hysteresis between forward and reverse sweeps of the transfer curves, as shown in Fig. 2(b), indicating that the device became more stable after Cytop modification. Fig. 5 shows electrical stability under negative bias gate stress for pentacene OFET. During the test, a negative gate bias ($V_G = -30$ V, $V_D = -30$ V) was applied as an electrical stress for 1 h, and the transfer curves were recorded every 15 min. The device without Cytop showed a threshold voltage shift of 5.1 V, while the one with Cytop showed a smaller shift of 2.8 V. Considering that the stress tests were performed in air condition without any encapsulation, the electrical stability of the OFET with Cytop was quite good. It is known that the OH groups at the insulator/semiconductor interface would cause device instability. There are no OH groups in the Cytop molecule, and the Cytop films are highly hydrophobic with a water contact angle of 106° which is better than those of many other polymers. Thus, the Cytop modification can passivate the large amounts of OH groups on the AlO_x:Nd surface, resulting in great improvement in the electrical stability.

To further evaluate bending flexibility of the metal–insulator–metal (MIM) and OFET device, bending tests were performed with the radius of curvature (R) from 50 to 10 mm for the outward bending and from −50 to −10 mm for the inward bending, as shown in the inset of Fig. 6. The leakage current density *versus* curvature (J–R) characteristics at a voltage of as high as 70 V of PEN/Al–Nd/AlO_x:Nd/Cytop/Au structure were shown in Fig. 6(a). The leakage current of this device was almost invariable (around 10^{-7} A cm^{-2}) even after bent to $|R| = 10$ mm under tension or compression, showing good bending flexibility and reliability of the Al–Nd/AlO_x:Nd/Cytop insulator. The breakdown curvature was about ±4 mm.

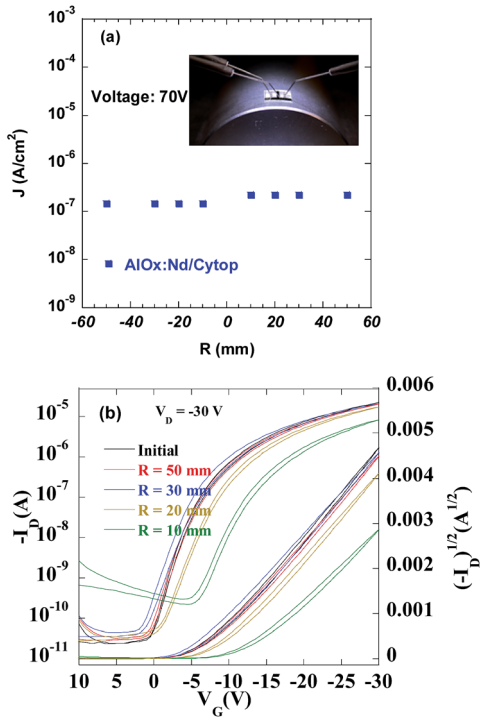

Fig. 6 (a) The leakage current density of AlO_x:Nd/Cytop *versus* curvatures; inset: the image of equipments in bending test. (b) Transfer characteristics of the flexible pentacene OFET under bending conditions; every curve includes forward (left) and reverse (right) sweeps.

The bending flexibility of the pentacene OFET with Cytop is shown in Fig. 6(b). The OFET device exhibited only small shifts in the transfer curves at bending curvatures larger than 20 mm, but the device decayed apparently with higher I_{off} and lower I_{on} after bent at $R = 10$ mm, which was attributed to the formation of cracks in the pentacene film. To further investigate the flexibility performance, the transfer curves for pentacene OFET with Cytop under bent to $|R| = 10$ mm, after 200 bending cycles were recorded (not shown). It was found that I_{on} became lower as the bending cycles increased, which may be attributed to the instability of pentacene in air condition. It was worth noting that there was slight increase in I_{off} after bent for more than 150 cycles, which may be due to the degradation of the AlO_x:Nd dielectric. The reason for the degradations are still under investigation.

Conclusions

In summary, flexible organic field-effect transistors (OFETs) with electrochemically oxidized gate insulators (AlO_x:Nd) were fabricated on a polyethylene naphthalate (PEN) substrate. The AlO_x:Nd insulator exhibited excellent insulating properties with low leakage current, high dielectric constant and high breakdown field. The surface of AlO_x:Nd was covered by Cytop. The surface roughness of AlO_x:Nd reduced from 4.1 to 1.4 nm after covered with Cytop. Meanwhile, the water contact angles were 66° and 106° before and after Cytop covering, respectively, implying lower surface energy after Cytop modification. The pentacene film on AlO_x:Nd without Cytop consisted of small grains with average grain size of ~200 nm, while the one with Cytop exhibited a dendritic structure with larger average grain size of ~350 nm. OFETs without Cytop exhibited a μ of 0.11 $cm^2 V^{-1} s^{-1}$, a V_{on} of −4 V, and an I_{on}/I_{off} of ~10^4, while the one with Cytop exhibited a higher μ of 0.75 $cm^2 V^{-1} s^{-1}$, a lower V_{on} of 0 V, and a higher I_{on}/I_{off} of ~10^6. The better performance of the Cytop-modified OFET was attributed to the smoother interface and larger grain size of the pentacene film. Furthermore, the Cytop-modified OFET showed much smaller hysteresis and better electrical stability under gate-bias stress (in air condition) compared to that without Cytop, which was ascribed to the hydroxyl-free nature of the Cytop molecule. In addition, the flexible OFET was able to maintain the relatively stable performance under a certain degree of bending. These results indicate that anodization represents a promising approach for flexible OFETs.

Acknowledgements

The authors are grateful to the National "863" Project of China (Grant no. 2014AA033002), the National Natural Science Foundation of China (Grant nos 61204087, 51173049, U0634003, and 60937001), the Zhujiang new science star project (Grant no. 2014J2200053), the Science and Technology Planning Project of Guangdong Province (Grant no. 2013B010403004), the Fundamental Research Funds for the Central Universities (Grant no. 2014ZM0003), and the Specialized Research Fund for the Doctoral Program of Higher Education (Grant no. 20120172120008).

Notes and references

1 A. Tsumura, H. Koezuka and T. Ando, *Appl. Phys. Lett.*, 1986, **75**, 1210.
2 C. D. A. M. Dimitrakopoulos, *Adv. Mater.*, 2002, **14**, 99.
3 L. A. Majewski, R. Schroeder and M. Grell, *Adv. Mater.*, 2005, **17**, 192.
4 T. Someya, A. Dodabalapur, J. Huang, K. C. See and H. E. Katz, *Adv. Mater.*, 2010, **22**, 3799.
5 J. S. Meena, M. Chu, R. Singh, C. Wu, U. Chand, H. You, P. Liu, H. D. Shieh and F. Ko, *RSC Adv.*, 2014, **4**, 18493.
6 Y. Zhu, T. Yin, J. Yin, N. Liu, Z. Yu, Y. Zhu, Y. Ding, J. Yin and Z. Wu, *RSC Adv.*, 2014, **4**, 40241.
7 H. Yang, C. Yang, S. H. Kim, M. Jang and C. E. Park, *ACS Appl. Mater. Interfaces*, 2010, **2**, 391.
8 A. N. Sokolov, B. C. Tee, C. J. Bettinger, J. B. H. Tok and Z. Bao, *Acc. Chem. Res.*, 2012, **45**, 361.
9 Y. Guo, G. Yu and Y. Liu, *Adv. Mater.*, 2010, **22**, 4427.
10 L. A. Majewski, M. Grell, S. D. Ogier and J. Veres, *Org. Electron.*, 2003, **4**, 27.
11 L. Lan and J. Peng, *IEEE Trans. Electron Devices*, 2011, **58**, 1452.
12 L. Lan, N. Xiong, P. Xiao, M. Li, H. Xu, R. Yao, S. Wen and J. Peng, *Appl. Phys. Lett.*, 2013, **102**, 242102.
13 L. A. Majewski, R. Schroeder and M. Grell, *J. Phys. D: Appl. Phys.*, 2004, **37**, 21.

14 H. Yang, C. Yang, S. H. Kim, M. Jang and C. E. Park, *ACS Appl. Mater. Interfaces*, 2010, **2**, 391.
15 C. Yang, K. Shin, S. Y. Yang, H. Jeon, D. Choi, D. S. Chung and C. E. Park, *Appl. Phys. Lett.*, 2006, **89**, 153508.
16 H. Klauk, M. Halik, U. Zschieschang, G. Schmid, W. Radlik and W. Weber, *J. Appl. Phys.*, 2002, **92**, 5259.
17 H. Xu, D. Luo, M. Li, M. Xu, J. Zou, H. Tao, L. Lan, L. Wang, J. Peng and Y. Cao, *J. Mater. Chem. C*, 2014, **2**, 1255.
18 L. Lan, M. Zhao, N. Xiong, P. Xiao, W. Shi, M. Xu and J. Peng, *IEEE Electron Device Lett.*, 2012, **33**, 827.
19 D. Luo, L. Lan, M. Xu, H. Xu, M. Li, L. Wang and J. Peng, *J. Electrochem. Soc.*, 2012, **159**, H502.
20 P. Xiao, L. Lan, T. Dong, Z. Lin, W. Shi, R. Yao, X. Zhu and J. Peng, *Appl. Phys. Lett.*, 2014, **104**, 51607.
21 L. Lan, J. Peng, M. Sun, J. Zhou, J. Zou, J. Wang and Y. Cao, *Org. Electron.*, 2009, **10**, 346.
22 J. Veres, S. D. Ogier, S. W. Leeming, D. C. Cupertino and S. MohialdinKhaffaf, *Adv. Funct. Mater.*, 2003, **13**, 199.
23 J. Veres, S. Ogier, G. Lloyd and D. de Leeuw, *Chem. Mater.*, 2004, **16**, 4543.
24 H. Sirringhaus, *Adv. Mater.*, 2005, **17**, 2411.
25 Z. Z. You and J. Y. Dong, *Appl. Surf. Sci.*, 2006, **253**, 2102.
26 S. Y. Yang, K. Shin and C. E. Park, *Adv. Funct. Mater.*, 2005, **15**, 1806.
27 S. Steudel, S. De Vusser, S. De Jonge, D. Janssen, S. Verlaak, J. Genoe and P. Heremans, *Appl. Phys. Lett.*, 2004, **85**, 4400.